DYNAMICS OF A THREE-DIMENSIONAL ASYMMETRIC INTERACTION OF DEFORMABLE BODIES WITH A RIGID WALL

V. A. Gorel'skii, I. E. Khorev, and N. T. Yugov

UDC 539.3

A number of experimental papers [1-4] have been devoted to the problem of the asymmetric interaction of deformable bodies during impact loading. The experimental research on three-dimensional flows is limited mainly to the recording of the final integral parameters of the process. The theoretical studies performed so far on three-dimensional flows which develop during impact loadings deal with the initial stage, and are descriptive in nature [5]. In the present article we use the method of finite elements [5-7] to treat numerically the three-dimensional problem of the interaction of a deformable body of revolution (cylinder) with a rigid wall for an impact velocity of 300 m/sec and angles of approach from 0 to 75°.

1. The equations which describe unsteady adiabatic motions of a solid compressible medium have the form

$$\rho dv_i/dt = \sigma_{ij,j}; \tag{1.1}$$

$$\partial\rho/\partial t + \operatorname{div}\rho v = 0; \tag{1.2}$$

$$dE/dt = (1/\rho)\sigma_{ij}\varepsilon_{ij}, \tag{1.3}$$

where $\sigma_{ij} = -P\delta_{ij} + S_{ij}$ are the components of the stress tensor, the ε_{ij} are the components of the strain-rate tensor, the v_i are the components of the velocity, ρ is the density, and E is the internal energy density.

The spherical part of the stress tensor is a function of the density and the internal energy:

$$P = \sum_{n=1}^{3} K_n\left(\frac{\rho}{\rho_0} - 1\right)^n\left[1 - K_0\left(\frac{\rho}{\rho_0} - 1\right)\Big/2\right] + K_0\rho_0 E_s \tag{1.4}$$

where K_n, ρ_0, and K_0 are material constants.

The deviatoric components of the stress tensor are found from the relation [8]

$$2G\left(\varepsilon_{ij} - \frac{1}{3}\varepsilon_{kk}\delta_{ij}\right) = \frac{dS_{ij}^0}{dt} + \lambda S_{ij} \tag{1.5}$$

where dS_{ij}^0/dt is the Jaumann derivative, defined by

$$dS_{ij}^0/dt = dS_{ij}/dt - S_{ik}W_{jk} - S_{jk}W_{ik}, \tag{1.6}$$

where $2W_{ij} = \partial v_i/\partial x_j - \partial v_j/\partial x_i$. The parameter λ is identically zero for elastic deformation, and for plastic deformation it is determined by using the Mises yield condition

$$S_{ij}S_{ij} = \frac{2}{3}\sigma_0^2. \tag{1.7}$$

Here G is the shear modulus and σ_0 is the dynamic yield stress.

2. We consider the problem of the impact of a deformable cylinder on a rigid wall. The velocity of the axisymmetric striker before impact coincides with its axis of symmetry and forms an angle α with the normal to the obstacle. The striker occupies the region D with the boundary R_1 and R_2, where R_1 is the contact boundary of the striker and the rigid obstacle, and R_2 is the free boundary of the striker. We pose the problem of solving Eqs. (1.1)-(1.7) with the following initial and boundary conditions:

Tomsk. Translated from Zhurnal Prikladnoi Mekhaniki i Tekhnicheskoi Fiziki, No. 4, pp. 112-118, July-August, 1985. Original article submitted April 17, 1984.

0021-8944/85/2604-0553$09.50

the initial conditions

$$\sigma_{ij}(0, x) = E(0, x) = 0,\ \rho(0, x) = \rho_0,$$
$$v_1(0, x) = 0,\ v_2(0, x) = -v_0 \sin\alpha,\ v_3(0, x) = -v_0 \cos\alpha \text{ for } x \in D. \tag{2.1}$$

the boundary condition on the free surface

$$T_{NN}(t, x) = T_{N\tau_1}(t, x) = T_{N\tau_2}(t, x) = 0 \quad \text{for} \quad x \in R_2. \tag{2.2}$$

the boundary condition on the surface of contact between the striker and the rigid wall – the condition of sliding without friction

$$T_{N\tau_1}(t, x) = T_{N\tau_2}(t, x) = 0, \quad v_N = 0 \quad \text{for} \quad x \in R_1, \tag{2.3}$$

where N is a unit vector normal to the surface at the point under consideration, τ_1 and τ_2 are perpendicular unit vectors in the plane tangent to the surface at the point under consideration, and T_N is the force per unit area on the surface with the normal N. In (2.2) and (2.3) the subscripts τ_1, τ_2, and N on the vectors T_N and v denote their projections on the corresponding basis vector.

3. We solve the above boundary-value problem by the method of finite elements [5, 7-9]. Using this method, we construct a discrete model of a body consisting of a finite number of finite elements appropriately connected at the corner points. The equation of motion for a typical finite element of a continuous medium is derived by using the principle of virtual velocities. Assuming that the mass of the elements is uniformly distributed over the nodes of the tetrahedral elements used in the calculations, the equation of motion for the whole ensemble of elements has the form [9]

$$m_k v'_{rk} = \sum_{l=1}^{L} \Omega_k^{n(l)} F_{rn}^{(l)}, \tag{3.1}$$

where m_k is the mass of the k-th node; v'_{rk} is the r-th component of the acceleration of the k-th node; and $F^{(\ell)}_{rn}$ is the r-th component of the equivalent force on the n-th node of the ℓ-th element. The elements of the body $\Omega^{n(\ell)}_k$ are defined in the following way:

$$\Omega_k^{n(l)} = \begin{cases} 1, & \text{if the n-th node of the } l\text{-th element corresponds to} \\ & \text{the k-th node of the associated model,} \\ 0 & \text{otherwise.} \end{cases}$$

The indices in (3.1) take on the following values: k = 1, 2, ..., M, where M is the number of nodes in the finite-element model of the cylinder; r = 1, 2, 3; n = 1, 2, 3, 4; ℓ = 1, 2, ..., L, where L is the total number of elements.

The energy equation for the ℓ-th element has the form

$$E'^{(l)} = (-P + Q)V'^{(l)} + V^{(l)} S_{ij} \varepsilon_{ij},$$

where $V^{(\ell)}$ is the relative volume of the element, and Q is the artifical viscosity.

The conservation of mass equation for an element is

$$(\rho/\rho_0)V^{(l)} = 1.$$

In accordance with the method of finite elements, the r-th component of the velocity within the ℓ-th tetrahedral element is expressed in terms of the four nodal values within the framework of the linear approximation assumed in the calculations by the formula

$$v_r^{(l)} = \frac{1}{6A^{(l)}}(a_n + b_n x_1 + c_n x_2 + d_n x_3) v_{rn}^{(l)}. \tag{3.2}$$

The coefficients appearing in (3.2) are determined in terms of the coordinates for each of the four nodes of the tetrahedral element, denoted by the indices p, q, s, and u:

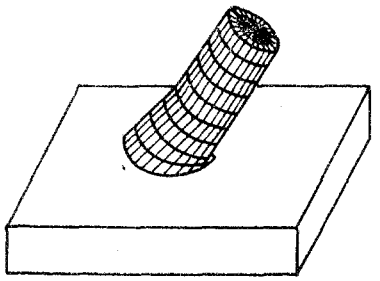

Fig. 1

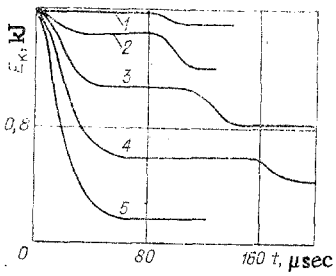

Fig. 2

$$A = \frac{1}{6}\begin{vmatrix} 1 & x_{1p} & x_{2p} & x_{3p} \\ 1 & x_{1q} & x_{2q} & x_{3q} \\ 1 & x_{1s} & x_{2s} & x_{3s} \\ 1 & x_{1u} & x_{2u} & x_{3u} \end{vmatrix}, \quad a_p = \begin{vmatrix} x_{1q} & x_{2q} & x_{3q} \\ x_{1s} & x_{2s} & x_{3s} \\ x_{1u} & x_{2u} & x_{3u} \end{vmatrix}, \tag{3.3}$$

$$b_p = \begin{vmatrix} 1 & x_{2q} & x_{3q} \\ 1 & x_{2s} & x_{3s} \\ 1 & x_{2u} & x_{3u} \end{vmatrix}, \quad c_p = \begin{vmatrix} 1 & x_{1q} & x_{3q} \\ 1 & x_{1s} & x_{3s} \\ 1 & x_{1u} & x_{3u} \end{vmatrix}, \quad d_p = \begin{vmatrix} 1 & x_{1q} & x_{2q} \\ 1 & x_{1s} & x_{2s} \\ 1 & x_{1u} & x_{2u} \end{vmatrix}.$$

The values of the remaining twelve coefficients are determined with the formulas given by the cyclic permutation of the indices. The strain rates within the ℓ-th element are calculated with the relation

$$\varepsilon_{ij}^{(l)} = \frac{1}{2}\left(\frac{\partial v_i^{(l)}}{\partial x_j} + \frac{\partial v_j^{(l)}}{\partial x_i}\right)$$

by using (3.2) and (3.3).

The components of the equivalent nodal forces appearing in Eq. (3.1) are found with the formulas

$$F_{1n} = -(1/6)(b_n\sigma_{11} + c_n\sigma_{12} + d_n\sigma_{13}),$$
$$F_{2n} = -(1/6)(c_n\sigma_{22} + b_n\sigma_{12} + d_n\sigma_{23}),$$
$$F_{3n} = -(1/6)(d_n\sigma_{33} + c_n\sigma_{23} + b_n\sigma_{13}).$$

In the numerical calculations we used the artificial viscosity [10]

$$Q = \begin{cases} \frac{1}{2}\rho a_0\left|\frac{V'}{V}\right| + 4\rho h^2\left|\frac{V'}{V}\right|^2, & \frac{V'}{V} < 0, \\ 0, & \frac{V'}{V} = 0, \end{cases}$$

where a_0 is the speed of sound in the material of the cylinder, and h is the minimum height of the tetrahedron.

The time increment in the integration which ensures a stable solution was determined from a numerical experiment, and has the form

$$\Delta t = \frac{4}{5}\left(\frac{h}{\sqrt{g^2} + \sqrt{g^2 + a_0^2}}\right), \quad g^2 = 4Q/\rho.$$

4. We investigated the interaction between a rigid wall and a steel cylinder 0.0125 m in diameter and having a length of three diameters. The velocity of the striker was 300 m/sec. The angle of impact was varied from 0 to 75°. The following numerical values of the material constants were used in the calculations: $\rho_0 = 7800$ kg/m^3, $a_0 = 5100$ m/sec, $\sigma_0 = 10.1\cdot10^8$ N/m^2, $G = 7.9\cdot10^{10}$ N/m^2, $K_1 = 1.53\cdot10^{11}$ N/m^2, $K_2 = 1.76\cdot10^{11}$ N/m^2, $K_3 = 0.532\cdot10^{11}$ N/m^2, $K_0 = 1.91$.

The interaction process was traced in detail by plotting striker configurations at successive instants. Figure 1 shows the configuration of the striker at 40 μsec for a 30° angle

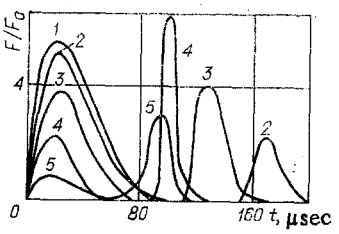

Fig. 3

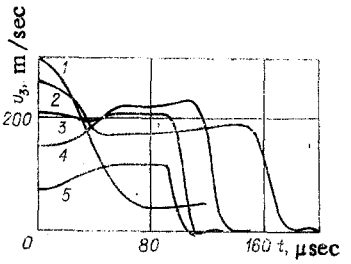

Fig. 4

of impact obtained with a graphical plotting device. The curves in Fig. 2 for the time dependence of the kinetic energy of the striker characterize the dynamics of the interaction in the range of impact angles investigated. Here and in the remaining figures, curves 5-1 correspond to angles of impact of 15, 30, 45, 60, and 75°. Analysis of the curves shows four main characteristic stages of the process. The first of these, characterized by a falloff of the curves, corresponds to the deformation of the head end of the cylinder, and is predominant for small angles of impact and unique for normal axisymmetric impact.

The following horizontal parts of the curves describe sliding of the cylinder along the wall of its simultaneous rotation and no noticeable deformation.

For 30-60° angles of impact there is a certain time interval during which the cylinder is not in contact with the obstacle. During this time the front part of the striker moves upward away from the wall, and the rear part moves downward toward the wall.

The second sharp decrease of kinetic energy was produced by the impact of the rear end of the cylinder with the obstacle. The graph shows that the drop in energy at this stage for a 45° angle of impact is approximately the same as for the interaction with the front part of the striker, and for angles of 60 and 75° even somewhat larger.

The final horizontal parts of the curves determine the sliding of the cylinder along the obstacle with a subsequent final withdrawal from it.

For a 15° angle of impact there is no second drop of kinetic energy. In this case the vertical component of the velocity of the center of mass of the striker changes sign at 70 μsec, and the cylinder begins gradually to withdraw from the wall. During this time it has an insignificant angular velocity. The center of mass practically coincides with the center of rotation. Up to the instant the rear end of the cylinder is at the bottom, the center of mass of the striker recedes from the obstacle to a distance greater than the distance from the center of rotation to the rear end of the cylinder, which passes over the obstacle without grazing it.

The graphs of the time variation of the forces of interaction of the striker with the wall shown in Fig. 3 for various angles of impact further characterize the multistage process described. The first maxima on the curves in Fig. 3 characterize the interaction of the front part of the cylinder with the obstacle. Then there are drops which for angles of 30, 45, and 60° reach zero. For an angle of 75° the cylinder–obstacle interaction does not vanish until the final withdrawal of the cylinder from the obstacle, which indicates continuous contact of the striker with the obstacle. The secondary maxima correspond to the impact of the rear end of the striker with the wall.

The graphs show that for an angle of 45° the force exerted on the obstacle during the impact of the rear end of the cylinder is comparable with the force exerted by the front part of the striker, and for angles of 60 and 75° even larger. This is accounted for by the increase of the vertical component of the velocity of the rear end of the cylinder as a result of rotation.

The time variations of the vertical component of the velocity of the center of the rear surface of the striker are shown in Fig. 4 for various angles of impact.

The slowing down of the rear surface is most pronounced for an angle of 15°. The velocity falls from an initial value of 290 m/sec to 40 m/sec in 80 μsec. Figure 5 shows that by this time the vertical component of the velocity of the center of mass has already changed sign and is directed upward from the obstacle. After 90 μsec the cylinder loses contact with the obstacle, and the striker moves upward and rotates, which results in a certain increase of the vertical velocity of the rear surface.

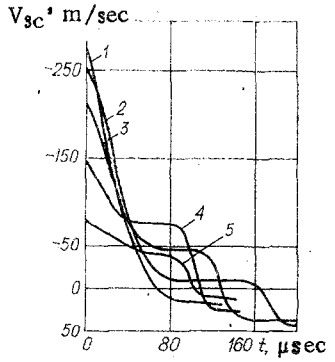

Fig. 5

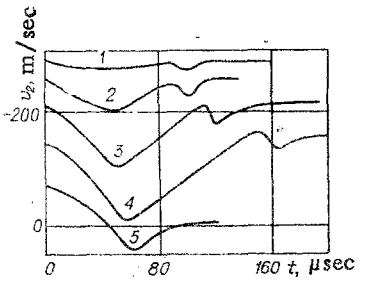

Fig. 6

For an angle of 30° the velocity drops from an initial value of 260 m/sec to 170 m/sec in 50 μsec. The front part of the cylinder is deformed and the striker is bent in the middle. The velocity is approximately constant and equal to 170 m/sec from 50 to 100 μsec, which corresponds to rotation and sliding of the cylinder along the rigid wall. This results in a redistribution of velocities such that the vertical component of the velocity of the center of the rear surface is constant, and the area of contact of the cylinder with the obstacle is decreased. During this time there is no further appreciable deformation of the front part of the cylinder. From 100 μsec the striker is not in contact with the obstacle. There is a certain increase of velocity during the withdrawal of the cylinder from the obstacle as a result of an increase of the angular velocity and the corresponding component of its linear velocity. From 120 to 150 μsec the striker moves in space and rotates. The part of the curve from 160 to 220 μsec corresponds to the impact of the rear end of the cylinder with the obstacle and its subsequent motion along it. Starting at 220 μsec the rear end of the cylinder separates from the wall, and the striker finally loses contact with the obstacle.

The curve for 45° differs quantitatively but not qualitatively from that for 30°. Thus, because of the increase in the angle of impact, the deformation of the front edge of the cylinder is more pronounced, and as a result the retardation of the rear surface and that of the whole striker is negligible. The vertical component of the velocity decreases from an initial value of 212 m/sec to 195 m/sec in 40 μsec. Then there is a small increase in the vertical velocity of the center of the rear surface when the deformation of the front part of the cylinder has largely ceased and the striker slides along the obstacle until t = 80 μsec. From this time on the front part of the striker separates from the wall, and for 30 μsec the cylinder moves in space without having contact with the obstacle. Between 110 and 180 μsec the rear end of the cylinder collides with the wall, is deformed, slides along it, and then separates from the obstacle, and from this time on moves away from it.

The character of the curve for an angle of 60° is somewhat different from those considered above. After the horizontal part extending from 0 to 10 μsec, which corresponds to a negligible deformation of the front edge of the cylinder, the curve rises, and in contrast with angles of 15, 30, and 45°, the front edge of the striker is deformed inward toward the axis. This increase is due to the rotation of the cylinder, which here is considerably more rapid than for smaller angles. The part of the curve from 50 to 90 μsec is flatter and corresponds to a decrease of the linear velocity during the rotation of the body as a result of the displacement of the center of rotation toward the rear end of the striker. From 90 to 110 μsec the rear part of the striker interacts with the obstacle. After this the cylinder separates from the wall, and the interaction stops. The curve for the variation of the vertical component of the velocity of the center of the rear surface for an angle of 75° is similar to the curve for 60°; therefore all the above is valid for it, too.

Calculations showed that the horizontal component of the velocity of the center of mass remains constant during the whole interaction process. This is a result of the boundary conditions given above, in which no restriction was imposed on the horizontal component of the velocity. Thus, only a redistribution of the horizontal components of the velocities at the nodes of the computational region can occur. The horizontal components of the velocity of the center of the rear surface of the striker for various angles of impact have the form shown in Fig. 6. The similarity of the curves further confirms the generality of the multistage process of the interaction of a cylinder with a rigid wall for various angles of impact.

The initial drops on the curves correspond to deformations of the front part of the striker and its bending, and are more or less pronounced depending on the angle of impact.

The subsequent rises of the curves correspond to sliding of the cylinder along the obstacle, accompanied by rotation. As the striker rotates and its rear end approaches the wall, the magnitude and direction of the horizontal component of the linear velocity change, which also is accounted for by the rise of the curves. Local minima on the curves corresponds to the impact of the end of the cylinder with the obstacle, and the following horizontal portions to sliding of the striker along the wall, followed by separation from it. It is clear from the figure that the horizontal velocity in these intervals is the same as the initial value.

Thus the asymmetric interaction of a deformable cylinder with a rigid wall occurs in several stages. Analysis of the results obtained shows four characteristic stages: deformation of the front part and bending of the striker; motion of the cylinder along the obstacle, accompanied by rotation; impact of the rear end with the obstacle, and its deformation; sliding of the striker along the wall, followed by separation from it. For different angles of impact these stages are more or less distinct qualitatively and quantitatively and in their duration.

In the range of initial conditions investigated, there were angles of impact between 60 and 75° for which the interaction mechanism changes qualitatively; for smaller angles there is a stage when there is no contact of the striker with the obstacle, even before the process has completely ended.

The authors thank V. G. Dulov for his attention to the work and a discussion of it.

LITERATURE CITED

1. V. M. Titov and Yu. I. Fadeenko, "Through penetration in meteorite impact," Kosm. Issled., 10, No. 4 (1972).
2. V. G. Dulov, V. A. Bordyug, et al., "Optimization of three-dimensional strikers," in: Papers of Seventh All-Union Conference on Numerical Methods of Solving Elasticity and Plasticity Theory Problems [in Russian], Novosibirsk (1982).
3. A. V. Utkin, A. N. Dremin, et al., "Characteristics of wave formation at large angles of impact of metal plates," Fiz. Goreniya Vzryva, No. 2 (1982).
4. I. E. Khorev, V. A. Gorel'skii, et al., "Deformation and kinetics of failure of contiguous bodies in an asymmetric dynamic interaction," Fiz. Goreniya Vzryva, No. 5 (1983).
5. G. R. Johnson, "High-velocity impact calculations in three dimensions," Trans. ASME, Ser. E, J. Appl. Mech., 44, 95-100 (1977).
6. I. E. Khorev and V. A. Gorel'skii, "Numerical modeling of split-off fractures in the axisymmetric interaction of solids," in: Detonation. Papers of the Second All-Union Conference on Detonation [in Russian], Chernogolovka, No. 2 (1981).
7. I. E. Khorev and V. A. Gorel'skii, "Axisymmetric splitting off in problems of the wide-range interaction," Dokl. Akad. Nauk SSSR, 271, No. 3 (1983).
8. S. S. Grigoryan, "On basic concepts in soil dynamics," Prikl. Mat. Mekh., 24, No. 6 (1960).
9. J. Oden, Finite Elements in the Mechanics of Continuous Media [Russian translation], Mir, Moscow (1976).
10. M. L. Wilkins, "Calculation of elastic–plastic flow," in: Computational Methods in Hydrodynamics [Russian translation], Mir, Moscow (1976).